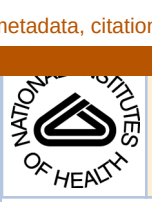

Published in final edited form as:

Circ Cardiovasc Imaging. 2009 May ; 2(3): 174–182. doi:10.1161/CIRCIMAGING.108.813766.

Adenosine Stress 64- and 256-Row Detector Computed Tomography Angiography and Perfusion Imaging A Pilot Study Evaluating the Transmural Extent of Perfusion Abnormalities to Predict Atherosclerosis Causing Myocardial Ischemia

Richard T. George, MD, **Armin Arbab-Zadeh, MD**, **Julie M. Miller, MD**, **Kakuya Kitagawa, MD**, **Hyuk-Jae Chang, MD**, **David A. Bluemke, MD, PhD**, **Lewis Becker, MD**, **Omair Yousuf, MD**, **John Texter, PA-C**, **Albert C. Lardo, PhD**, and **João A.C. Lima, MD**

Department of Medicine, Division of Cardiology (R.T.G., A.A.-Z., J.M.M., K.K., H.-J.C., D.A.B., L.B., O.Y., J.T., A.C.L., J.A.C.L.), Department of Biomedical Engineering (A.C.L.), and Department of Radiology (D.A.B., J.A.C.L.), Johns Hopkins University School of Medicine, Baltimore, Md.

Abstract

Background—Multidetector computed tomography coronary angiography (CTA) is a robust method for the noninvasive diagnosis of coronary artery disease. However, in its current form, CTA is limited in its prediction of myocardial ischemia. The purpose of this study was to test whether adenosine stress computed tomography myocardial perfusion imaging (CTP), when added to CTA, can predict perfusion abnormalities caused by obstructive atherosclerosis.

Methods and Results—Forty patients with a history of abnormal single-photon emission computed tomography myocardial perfusion imaging (SPECT-MPI) underwent adenosine stress 64-row (n=24) or 256-row (n=16) detector CTP and CTA. A subset of 27 patients had invasive angiography available for quantitative coronary angiography. CTA and quantitative coronary angiography were evaluated for stenoses ≥50%, and SPECT-MPI was evaluated for fixed and reversible perfusion deficits using a 17-segment model. CTP images were analyzed for the transmural differences in perfusion using the transmural perfusion ratio (subendocardial attenuation density/subepicardial attenuation density). The sensitivity, specificity, positive predictive value, and negative predictive value for the combination of CTA and CTP to detect obstructive atherosclerosis causing perfusion abnormalities using the combination of quantitative coronary angiography and SPECT as the gold standard was 86%, 92%, 92%, and 85% in the per-patient analysis and 79%, 91%, 75%, and 92% in the per vessel/territory analysis, respectively.

Conclusions—The combination of CTA and CTP can detect atherosclerosis causing perfusion abnormalities when compared with the combination of quantitative coronary angiography and SPECT.

Correspondence to João A.C. Lima, MD, Johns Hopkins University, Department of Medicine, Division of Cardiology, 600 N Wolfe St, 524 Blalock Bldg, Baltimore, MD 21287. jlima@jhmi.edu.

Disclosures: Drs George, Miller, Lardo, and Lima are, in part, funded by a research grant from Toshiba Medical Systems Inc. Drs George, Lardo, and Kitagawa report receiving honoraria from Toshiba to lecture on cardiovascular CT. The terms of this arrangement are being managed by the Johns Hopkins University in accordance with its conflict-of-interest policies.

Keywords

imaging; atherosclerosis; ischemia; perfusion; myocardium

Computed tomography noninvasive coronary angiography (CTA) using 64-detector technology has been shown to compare well with invasive coronary angiography,[1] and multiple studies have shown that CTA has a negative predictive value (NPV) of 95% to 99%, therefore superseding all other noninvasive imaging modalities in its ability to exclude coronary artery disease (CAD).2,3 However, multidetector CTA provides no information on the physiological significance of coronary atherosclerosis. To date, several studies have shown that a 50% stenosis identified by CTA is a poor predictor of reversible ischemia.4–6

For patients with moderate to severe coronary stenosis, it is thus desirable to measure myocardial perfusion in conjunction with the extent of luminal stenosis. One approach is to combine CTA with radionuclide myocardial perfusion imaging (MPI), a strategy that requires the combination of 2 separate imaging technologies.[4] Alternatively, we have previously demonstrated in preclinical studies that CT technology alone is capable of simultaneous atherosclerosis and myocardial perfusion measurements.7,8 Importantly, high-resolution CT, in contrast to radionuclide MPI, has the potential of assessing the transmural extent of myocardial perfusion abnormalities similar to MRI.9,10 Finally, the recent introduction of dynamic volume CT with 256 and 320 detectors has enabled the performance of CTA11,[12] with temporal uniformity (ability to image the entire heart simultaneously) and lower radiation, thus enabling combined measurements of anatomy and perfusion during rest and stress as part of a single diagnostic examination.

The primary objective of this study was to determine whether adenosine stress CT perfusion (CTP) imaging, in conjunction with CTA, can detect atherosclerosis causing myocardial perfusion abnormalities. Specifically, we tested the hypothesis that adenosine stress CT-derived transmural perfusion measurements are predictive of myocardial perfusion abnormalities in the setting of obstructive atherosclerosis.

Methods

Patient Selection

The study protocol was reviewed and approved by the Johns Hopkins University Institutional Review Board, and all patients signed written informed consent. Patients were enrolled from January 2006 to August 2007. The study included men and nonpregnant women with a clinical suspicion of CAD and history of an abnormal single-photon emission computed tomography (SPECT) MPI within the past 60 days. Exclusion criteria included history of renal insufficiency, contraindications to iodinated contrast, atrial fibrillation, bronchospastic lung disease, and 2nd- or 3rd-degree heart block. Patients underwent CTA and perfusion imaging within 60 days after SPECT MPI. Twenty-seven patients subsequently underwent invasive coronary angiography.

SPECT Imaging and Analysis

In all patients, stress-rest MPI (using either technetium-99m tetrofosmin or technetium-99m sestamibi) was performed with symptom-limited treadmill exercise or pharmacological (dipyridamole or adenosine) stress according to protocols endorsed by the American Society of Nuclear Cardiology.[13] Gated and nongated SPECT image data were reconstructed in the vertical long-axis, horizontal long-axis, and short-axis projections. Using a 17-segment model, a single blinded observer visually scored myocardial segments as normal, mild,

moderate, or severe, and reversibility was determined. Perfusion deficits were assigned a culprit vessel.14

CTA and Perfusion Image Acquisition and Reconstruction

Baseline blood pressure (BP), heart rate (HR), and ECG were acquired before CT. Oral and/or intravenous metoprolol was given if the resting HR was >65 beats per minute. Intravenous access was obtained in the right and left antecubital veins for the administration of iodinated contrast and adenosine, respectively. Patients were hydrated with 250 to 500 mL normal saline before CT imaging.

64-Detector CT

Patients were placed supine in a 64-row detector CT (64-DCT) scanner (Aquilion 64, Toshiba Medical Systems, Nasu, Japan). After the acquisition of scout images, adenosine (0.14 mg/kg/min; Adenoscan, Astellas Pharma US, Deerfield, Ill) was initiated with continuous ECG monitoring. Five minutes into the adenosine infusion, iodinated contrast (Iopamidol, 370 mg I/mL; Bracco Diagnostics, Princeton, NJ) was infused at a rate of 5 mL/s for a total of 90 to 95 mL, followed by 30 mL of normal saline. The contrast bolus was monitored using the automated bolus tracking feature and CT imaging was initiated when a threshold of 150 Hounsfield units (HU) was detected in the left ventricular blood pool according to a retrospective ECG-gated protocol with the following parameters: detector collimation, 64×0.5 mm; tube current, 400 mA; tube voltage, 120 kV; gantry rotation time, 400 ms; beam pitch, variable depending on HR (Figure 1). Effective radiation dose estimated using the dose-length product method was 16.8 mSv for 64-DCT imaging.

CT raw data were reconstructed for angiographic analysis as previously described.[1] For the analysis of perfusion, images were reconstructed in the cardiac short axis with a 3.0-mm slice thickness at end diastole (phase 80% to 100%), selecting the phase with the least cardiac motion using a standard body algorithm kernel (FC13) without edge enhancement.

256-Detector CT

Patients were placed supine in a 256-row detector CT (256-DCT) prototype scanner (TSX-301A, Aquilion One CT System, Toshiba Medical Systems). After the acquisition of scout images, a test bolus of iodinated contrast (Iopamidol, 370 mg I/mL; Bracco Diagnostics) was infused at 5 mL/s for a total of 20 mL, and bolus tracking imaging was performed to determine scan timing.

256-Stress CTP Imaging

Adenosine was initiated with continuous ECG monitoring. Five minutes into the adenosine infusion, iodinated contrast was infused at a rate of 5 mL/s in 2 phases: 100% contrast for 50 mL, then a 50:50 mixture of contrast and saline for 20 mL, followed by 30 mL of normal saline (total contrast, 60 mL). CT imaging was initiated at the predicted peak of the contrast bolus. CT settings were as follows: detector collimation, 128×1.0 mm; tube current, 200 mA; tube voltage, 120 kV; gantry rotation time, 500 ms; and scan time, 1.5 seconds.

Stress CTP images were reconstructed in the short axis with a 3-mm slice thickness at end diastole (phase 80% to 100%), selecting the phase with the least cardiac motion. Images were reconstructed with the same standard body algorithm kernel (FC13) with beam-hardening correction and without edge enhancement.

256-Rest CTA and Perfusion Imaging

Ten minutes after stress CTP imaging, the CT angiogram and rest perfusion imaging were acquired. Iopamidol was infused using the same protocol for stress CTP (total contrast, 60 mL). CT imaging was initiated at the predicted peak of the contrast bolus. CT settings were as follows: detector collimation, 256× 0.5 mm; tube current, 350 mA; tube voltage, 120 kV; gantry rotation time, 500 ms; and scan time, 1.5 seconds. Effective radiation dose estimated using the dose length product method was 21.6 mSv for rest and stress 256-DCT imaging combined.

CT angiograms were reconstructed with a 0.5-mm slice thickness using half-scan reconstruction with standard (FC43) CTA and sharp (FC05) kernels using the phase with least cardiac motion.

For rest perfusion analysis in the 256-DCT group, images were reconstructed in the short axis with a 3-mm slice thickness at end diastole (phase 80% to 100%), selecting the phase with the least cardiac motion using the same standard body algorithm kernel (FC13) with beam-hardening correction and without edge enhancement.

CT Myocardial Perfusion Image Analysis

CT stress (64 and 256-DCT) and rest (256-CT only) images were transferred to a custom myocardial perfusion analysis workstation (Toshiba Medical Systems). Using images in the cardiac short axis with a 3-mm slice thickness, 2 independent and blinded observers (1 cardiologist and 1 radiologist) analyzed the CTP images as follows: (1) Using an automated border detection algorithm with manual hand planimetry input, the subendocardial and subepicardial borders were defined; (2) the software automatically and equally divided the myocardium into three myocardial layers: the subendocardial, midmyocardial, and subepicardial layers; and (3) using a 16-segment model (apex was excluded), the software calculated the mean attenuation density (AD) of each myocardial layer within each sector (Figure 2).

To calculate the transmural extent of perfusion abnormalities in a quantitative analysis, the transmural perfusion ratio was calculated as follows:

$$TPR = \frac{Subendocardial \quad AD}{Subepicardial \quad AD}$$

where TPR=transmural perfusion ratio, subendocardial AD is the sector specific subendocardial attenuation, and subepicardial AD is the mean attenuation of the entire subepicardial layer of any given short-axis slice. The TPR was calculated for each segment. Interobserver variability in the measurement of the TPR was performed by comparing the results from the 2 blinded readers on a segment-by-segment basis. The final TPR result used in the analysis was the average TPR from both readers.

CT Coronary Angiography Analysis

CT angiographic images were transferred to a dedicated workstation (Vitrea v. 3.9, Vital Images, Minnetonka, Minn) for analysis by a level III certified CT angiographer. All segments ≥1.5 mm were analyzed regardless of the presence of intracoronary stents or coronary calcification using a 19-segment coronary model.[15] Each coronary segment was visually assessed for the percent luminal stenosis and a vessel supplying a territory was considered obstructive if there was at least 1 segment of a vessel with a ≥50% luminal stenosis.

Invasive Coronary Angiography Acquisition and Quantitative Coronary Analysis

Invasive coronary angiography (ICA) was performed using standard orthogonal views and was clinically driven. Coronary angiographic images were transferred to an independent angiographic core laboratory for analysis. The coronary tree was analyzed using a 19-segment coronary model as previously described.[15] Quantitative coronary angiography (QCA) was performed on all coronary segments >1.5 mm in diameter (CAAS II QCA Research version 2.0.1 software, PIE Medical Imaging, Maastricht, The Netherlands) on the most significant stenosis ≥30% severity within each coronary segment. A vessel supplying a territory was considered obstructive if at least 1 segment of a vessel contained a ≥50% luminal stenosis.

Hybridization of Multimodality Imaging

Perfusion deficits noted on CTP and SPECT MPI were assigned a coronary artery territory according to standard practice.[14] In cases in which variation of the coronary arterial anatomy varied from standard practice, the CTA was used to reassign segments to the appropriate vessel territory for both SPECT and CTP in the following way: (1) the anterolateral wall was assigned to the left anterior descending artery (LAD) territory if there was a diagonal vessel overlying the anterolateral wall, (2) the distal inferior wall was assigned to the LAD if the LAD wrapped around the apex and supplied the distal inferior wall, and (3) the inferolateral wall was assigned to the right coronary artery (RCA) territory if the RCA supplied a posterolateral branch overlying the inferolateral wall.

In the patient-based analysis, CTA/CTP and QCA/SPECT were considered positive when CTA or QCA showed a ≥50% luminal stenosis and a perfusion deficit. In the vessel/territory-based analysis, CTA/CTP and QCA/SPECT were considered positive when CTA or QCA showed a ≥50% luminal stenosis in a vessel supplying a territory with a perfusion deficit.

Because SPECT is limited in the evaluation of patients with 3-vessel and left main CAD, a separate analysis was performed to avoid penalizing CTP for detecting multivessel disease in the vessel/territory analysis.[16] In those patients with 3-vessel or left main disease (confirmed by QCA), if CTA/CTP and QCA/SPECT showed 1 territory supplied by a ≥50% stenosis in the presence of a matching perfusion deficit, yet CTA/CTP showed a second or third territory to have a ≥50% stenosis in the presence of a matching perfusion deficit missed by SPECT, CTA/CTP was not penalized for finding the second or third territories.

Statistical Analysis

Means are expressed as ±SD. Interobserver variability was compared using Bland-Altman plots and the κ statistic, respectively.[17,18] The relationship between percent luminal stenosis and TPR was compared using Pearson correlation. The mean TPR at each level of stenosis was compared using 1-way analysis of variance. The area under the receiver operating characteristic (ROC) was calculated and reported with 95% confidence intervals.[19] The threshold of significance was $P<0.05$. Statistical analyses were performed using Med-Calc version 8.2.1.0 (Meriakerke, Belgium).

Results

Forty-three consecutive patients underwent 64 (n=24) or 256 (n=19) CT imaging. The first 3 patients from the 256-DCT group underwent developmental protocols and were excluded from the analysis. Myocardial perfusion imaging by CT was compared with SPECT MPI in a total of 40 patients, 120 territories, and 640 sectors. ICA was performed in 27 of 40 patients. Baseline characteristics are shown in Table 1. Mean HR was 138.8±18.5,

101.7±9.5, and 75.4±12.9, and mean systolic BP was 173.4±27.2, 134.3±14.3, and 123.1±18.2 during peak exercise SPECT, pharmacological SPECT, and stress CTP; respectively.

CT Transmural Perfusion Ratio and Percent Stenosis by QCA

Among 14 patients with no obstructive epicardial coronary disease on QCA (no stenoses ≥30%), 224 myocardial segments were analyzed to define the normal distribution of the TPR, Figure 3. The mean±SD TPR was 1.12±0.13 in these patients with no obstructive CAD. The TPR was considered abnormal when it was <0.99 or more than 1 SD below the mean TPR in this group of normal patients.

Interobserver variability for measuring segmental TPR was good (κ=0.72; 95% CI, 0.63 to 0.802 and κ=0.63; 95% CI, 0.56 to 0.70) for the rest and stress images, respectively.[17] The agreement between measurements of segmental TPR was good on rest and stress imaging (Figure 4).

The transmural perfusion ratio for stenoses of 30% to 49%, 50% to 69%, and 70% to 100% severity on QCA was 1.09±0.11, 1.06±0.14, and 0.91±0.10 respectively (TPR for 70% to 100% stenoses was significantly lower compared with stenoses of 30% to 49% and 50% to 69%, P<0.001). There was a significant inverse linear correlation between the TPR and the percent diameter stenosis (R=–0.63, P=0.001, Figure 5.

CT Angiography/CT Perfusion Versus QCA/SPECT Perfusion Imaging

Figure 6 and Figure 7 demonstrate examples of CTP imaging with 64- and 256-DCT, respectively. One patient was excluded from the analysis secondary to an uninterpretable CTA. The sensitivity, specificity, positive predictive value (PPV), and NPV for CTA/CTP detecting a stenosis causing a perfusion deficit on QCA/SPECT was 86%, 92%, 92%, and 85% in the patient-based analysis and 75%, 87%, 60%, and 93% in the vessel/territory based analysis, respectively (Table 2 and Table 3).

QCA demonstrated 1-, 2-, and 3- vessel disease in 30.8%, 19.2%, and 7.7% of patients, respectively. When taking into consideration that CTP detects perfusion deficits in a second or third territory in patients with 3-vessel or left main disease the sensitivity, specificity, PPV, and NPV of CTA/CTP, when compared with QCA/SPECT was 79%, 91%, 75%, and 93% in the per vessel/territory based analysis (Table 3).

CT Perfusion versus SPECT Perfusion and Reversibility

During stress imaging, perfusion deficit extent was 3.8±2.4 and 3.8±3.7 sectors on SPECT and CTP imaging, respectively (P=0.91). On a territorial/vessel-based analysis, the sensitivity, specificity, PPV, and NPV for CTP detecting a SPECT perfusion deficit was 70%, 51%, 58%, and 63%, respectively.

In the 256-row CT group, in which both rest and stress perfusion on SPECT and CT imaging were available, 1 patient with a normal SPECT study had a partially reversible defect on CTP. There were 6 patients with reversible perfusion deficits on SPECT with CTP deficits noted to be reversible in 2 patients, partially reversible in 1 patient, and fixed in 3 patients. All 7 patients noted to have partially reversible perfusion deficits on SPECT also had partially reversible perfusion deficits on CT. Two patients with fixed deficits on SPECT had partially reversible perfusion deficits on CTP.

Discussion

This study is the first to quantify transmural differences of myocardial perfusion by CT in humans. Its main findings are (1) adenosine stress CTP imaging can detect transmural differences in myocardial perfusion; (2) these transmural differences in the subendocardial and subepicardial attenuation can be quantified using the TPR; (3) TPR is inversely related to percent diameter stenosis measured by quantitative angiography; (4) severe CTP deficits indicate the presence of severe stenoses detected by invasive angiography; and (5) CTP, when combined with CTA, can accurately predict coronary stenosis causing perfusion deficits on QCA/SPECT.

Angiography Versus Myocardial Perfusion

Previous studies have established that coronary angiography and MPI provide quite different but complimentary assessments of ischemic heart disease. Although invasive coronary angiography has the advantage of directly visualizing and quantifying the severity of coronary stenoses caused by atherosclerosis, metrics such as percent diameter stenosis have been shown to only moderately correlate with measurements of myocardial perfusion using positron-emission tomography (PET) and fractional flow reserve.[20,21] Furthermore, radionuclide MPI has been shown to have incremental prognostic value when used in conjunction with, and independent of, the coronary angiogram.[22,23]

Although CTA provides a noninvasive assessment of percent diameter stenosis and allows for the identification of atherosclerotic plaque, it falls short of providing information on the physiological significance of coronary stenoses.[4–6] Furthermore, a recent study has demonstrated that overall plaque burden on CTA, rather than plaque location, is a better predictor of territorial ischemia on radionuclide MPI.[24] Preferably, noninvasive testing for CAD would assess atherosclerosis and perfusion imaging in 1 setting. There are several prospects for this comprehensive evaluation of ischemic heart disease, including hybrid imaging systems that combine CTA with SPECT or PET.[4,6] However, these systems come with additional cost and, in some instances, significant increases in the overall radiation dose.[4] Our study, in conjunction with several preclinical studies of CTP imaging by our group and others, proposes the concept that CT alone can provide simultaneous atherosclerosis and MPI.[7,8,25]

Transmural Distribution of Myocardial Perfusion

SPECT MPI using technetium- and thallium-based radionuclide tracers are well established for the evaluation of myocardial perfusion. However, due to limited spatial resolution, SPECT is not capable of detecting transmural differences in myocardial perfusion. Although improvements in spatial resolution are seen with PET, which is actually capable of quantifying myocardial perfusion, PET still falls short of enabling quantification of the transmural extent of myocardial perfusion. In this regard, MRI is the only other modality capable of visualizing transmural differences in myocardial perfusion, even if limited in allowing for its accurate quantification.[9,10,26]

It is well established that the first manifestations of myocardial ischemia occur in the subendocardium.27 Under resting conditions, in the absence of critical CAD, myocardial perfusion is higher in the subendocardium than in the subepicardium.[9,28] Whereas this endocardial/epicardial flow ratio is maintained in myocardium supplied by normal epicardial arteries during the administration of vasodilators (ie, dipyridamole and adenosine), it is decreased in myocardium supplied by stenosed epicardial arteries. Previously, Keijer et al used gadolinium-enhanced MR perfusion imaging to measure relative transmural differences in myocardial perfusion clinically. During dipyridamole stress MRI, they demonstrated

subendocardial/subepicardial ratios of 1.08±0.23 in normal territories and 0.96±0.21 in abnormal territories supplied by vessels with diameter stenoses ranging from 70% to 99%. These finding are very similar to our findings of TPR=1.12±0.13 in territories supplied by normal coronary arteries and our finding of TPR=0.91±0.10 in territories supplied by coronary arteries with 70% to 100% diameter stenoses.

Helical Versus Dynamic Volume CT

In this study, patients were imaged on either a 64-DCT or a 256-DCT system. It is important to point out that the 256-DCT system used in this study was a prototype 256 system and commercially available 320-row detector systems that provide similar dynamic volume CT capabilities have since been introduced. Although the current study was not designed to compare the efficacy of 64- versus 256-DCT scanners for CTP imaging, there are several potential advantages that full cardiac coverage with dynamic volume (256- to 320-row detector) CT scanning can provide. Current radiation and contrast doses limit the ability to perform rest and stress studies. The ability to perform a rest study is important to ensure a high-quality CTA and to assess the reversibility of a perfusion deficit. The recent introduction of prospective ECG gating has significantly reduced the overall radiation dose for CTA and is currently available on 64- and 320-detector systems. However, prospective ECG gating with 64-DCT is limited in temporal resolution due to half-scan reconstruction, limiting its use to patients with HR <63 beats per minute.[29] In the current study, the mean HR during adenosine infusion was 75 beats per minute. Alternatively, prospective ECG gating with dynamic volume CT is capable of segmented reconstruction and thus will allow imaging at the higher HRs commonly experienced during adenosine infusion. 320-DCT is also capable of synchronous perfusion imaging of the entire heart. At the present time, it is unclear whether imaging the base of the heart at a different time than the apex may impact the evaluation of myocardial perfusion by CT within a patient.

Limitations

There are several limitations to this study in regard to study design and inherent limitations of CT technology for the assessment of myocardial perfusion. First, this was a study of patients with mostly abnormal SPECT studies, therefore limited in its assessment of CTP imaging in patients with normal perfusion. However, the study does show that the TPR in those patients with normal coronary arteries on QCA did indeed have a normal TPR on CTP imaging. Second, this study only used rest perfusion imaging in the 256-DCT group; therefore no assessment of reversibility was available in the 64-DCT group. Further, this study used patients from the study group to establish a cutoff for an abnormal TPR. Therefore, further validation studies are required to confirm these promising results.

The 256-DCT scanner used in this study was a prototype scanner. This prototype scanner was limited in temporal resolution and did not have prospective ECG gating available. Therefore, the radiation dose in this study was relatively high compared with the low-dose CT protocols currently available on the 320-row detector scanner.

Moreover, CTA frequently uses β-blockers to lower the HR. β-Blockers have been shown to increase hyperemic myocardial blood flow, and this effect may reduce differences between normally perfused and ischemic territories.[30] In this regard, β-blockers may have “hidden” ischemia in 1 patient with significant CAD whose HR remained below 60 beats per minute during adenosine infusion. Last, beam-hardening artifacts can be mistaken for myocardial perfusion deficits. For the purposes of this study, we developed a beam-hardening correction that was implemented to correct for artifacts during reconstruction of the dynamic volume CT studies.[31]

Conclusions

CTP imaging can detect transmural differences in myocardial perfusion that can be accurately quantified as the transmural perfusion ratio (subendocardial/subepicardial attenuation density). CTP imaging, when combined with CTA, can accurately predict atherosclerosis causing perfusion abnormalities in comparison with combined QCA/SPECT. The combination of CTA with CTP imaging could have ground-breaking implications to the future diagnostic evaluation of patients with suspected CAD.

CLINICAL PERSPECTIVE

Multidetector computed tomography coronary angiography (CTA) is a robust method for the noninvasive diagnosis of coronary artery disease. However, in its current form, CTA is limited in its prediction of myocardial ischemia. This pilot study investigated whether the combination for CTA and adenosine stress CT myocardial perfusion imaging can accurately detect atherosclerosis, causing perfusion abnormalities compared with the combination of invasive angiography and single-photon emission computed tomography. In a quantitative analysis, CT perfusion images were analyzed for the transmural perfusion ratio, the ratio of the subendocardial attenuation density, and the subepicardial attenuation density. This study demonstrated that CT perfusion imaging, when performed with adenosine, can detect subendocardial perfusion deficits and the combination of CTA and CT perfusion imaging can detect obstructive atherosclerosis causing perfusion abnormalities when compared with the combined gold standard of invasive angiography and single-photon emission computed tomography myocardial perfusion imaging. If confirmed by larger studies, the combination of CTA with CT perfusion imaging could have important implications to the future diagnostic evaluation of patients with suspected coronary artery disease.

Acknowledgments

We thank Jorge Guzman, Theresa Caton, and Katherine Hannon for technical assistance.

Sources of Funding: This study was supported by an American College of Cardiology Foundation Career Development Award, a Donald W. Reynolds Foundation Clinical Cardiovascular Research Center Award, Toshiba Medical Systems Corporation and Astellas Pharma US, Inc, and the PJ Schafer Memorial Research Grant.

References

1. Miller JM, Rochitte CE, Dewey M, Arbab-Zadeh A, Niinuma H, Gottlieb I, Paul N, Clouse ME, Shapiro EP, Hoe J, Lardo AC, Bush DE, de Roos A, Cox C, Brinker J, Lima JA. Diagnostic performance of coronary angiography by 64-row CT. N Engl J Med 2008;359:2324–2336. [PubMed: 19038879]
2. Budoff MJ, Dowe D, Jollis JG, Gitter M, Sutherland J, Halamert E, Scherer M, Bellinger R, Martin A, Benton R, Delago A, Min JK. Diagnostic performance of 64-multidetector row coronary computed tomographic angiography for evaluation of coronary artery stenosis in individuals without known coronary artery disease: results from the prospective multicenter ACCURACY (Assessment by Coronary Computed Tomographic Angiography of Individuals Undergoing Invasive Coronary Angiography) trial. J Am Coll Cardiol 2008;52:1724–1732. [PubMed: 19007693]
3. Vanhoenacker PK, Heijenbrok-Kal MH, Van Heste R, Decramer I, Van Hoe LR, Wijns W, Hunink MG. Diagnostic performance of multidetector CT angiography for assessment of coronary artery disease: meta-analysis. Radiology 2007;244:419–428. [PubMed: 17641365]
4. Rispler S, Keidar Z, Ghersin E, Roguin A, Soil A, Dragu R, Litmanovich D, Frenkel A, Aronson D, Engel A, Beyar R, Israel O. Integrated single-photon emission computed tomography and computed

tomography coronary angiography for the assessment of hemodynamically significant coronary artery lesions. J Am Coll Cardiol 2007;49:1059–1067. [PubMed: 17349885]

5. Schuijf JD, Wijns W, Jukema JW, Atsma DE, de Roos A, Lamb HJ, Stokkel MP, Dibbets-Schneider P, Decramer I, De Bondt P, van der Wall EE, Vanhoenacker PK, Bax JJ. Relationship between noninvasive coronary angiography with multi-slice computed tomography and myocardial perfusion imaging. J Am Coll Cardiol 2006;48:2508–2514. [PubMed: 17174190]
6. Di Carli MF, Dorbala S, Curillova Z, Kwong RJ, Goldhaber SZ, Rybicki FJ, Hachamovitch R. Relationship between CT coronary angiography and stress perfusion imaging in patients with suspected ischemic heart disease assessed by integrated PET-CT imaging. J Nucl Cardiol 2007;14:799–809. [PubMed: 18022106]
7. George RT, Jerosch-Herold M, Silva C, Kitagawa K, Bluemke DA, Lima JA, Lardo AC. Quantification of myocardial perfusion using dynamic 64-detector computed tomography. Invest Radiol 2007;42:815–822. [PubMed: 18007153]
8. George RT, Silva C, Cordeiro MA, DiPaula A, Thompson DR, McCarthy WF, Ichihara T, Lima JA, Lardo AC. Multidetector computed tomography myocardial perfusion imaging during adenosine stress. J Am Coll Cardiol 2006;48:153–160. [PubMed: 16814661]
9. Keijer JT, van Rossum AC, van Eenige MJ, Bax JJ, Visser FC, Teule JJ, Visser CA. Magnetic resonance imaging of regional myocardial perfusion in patients with single-vessel coronary artery disease: quantitative comparison with (201)Thallium-SPECT and coronary angiography. J Magn Reson Imaging 2000;11:607–615. [PubMed: 10862059]
10. Christian TF, Rettmann DW, Aletras AH, Liao SL, Taylor JL, Balaban RS, Arai AE. Absolute myocardial perfusion in canines measured by using dual-bolus first-pass MR imaging. Radiology 2004;232:677–684. [PubMed: 15284436]
11. Motoyama S, Anno H, Sarai M, Sato T, Sanda Y, Ozaki Y, Mochizuki T, Katada K, Hishida H. Noninvasive coronary angiography with a prototype 256-row area detector computed tomography system: comparison with conventional invasive coronary angiography. J Am Coll Cardiol 2008;51:773–775. [PubMed: 18279744]
12. Rybicki FJ, Otero HJ, Steigner ML, Vorobiof G, Nallamshetty L, Mitsouras D, Ersoy H, Mather RT, Judy PF, Cai T, Coyner K, Schultz K, Whitmore AG, Di Carli MF. Initial evaluation of coronary images from 320-detector row computed tomography. Int J Cardiovasc Imaging 2008;24:535–546. [PubMed: 18368512]
13. Imaging guidelines for nuclear cardiology procedures, part 2: American Society of Nuclear Cardiology. J Nucl Cardiol 1999;6:G47–G84. [PubMed: 10327112]
14. Cerqueira MD, Weissman NJ, Dilsizian V, Jacobs AK, Kaul S, Laskey WK, Pennell DJ, Rumberger JA, Ryan T, Verani MS. Standardized myocardial segmentation and nomenclature for tomographic imaging of the heart: a statement for healthcare professionals from the Cardiac Imaging Committee of the Council on Clinical Cardiology of the Am Heart Association. Circulation 2002;105:539–542. [PubMed: 11815441]
15. Miller JM, Dewey M, Vavere AL, Rochitte CE, Niinuma H, Arbab-Zadeh A, Paul N, Hoe J, de Roos A, Yoshioka K, Lemos PA, Bush DE, Lardo AC, Texter J, Brinker J, Cox C, Clouse ME, Lima JA. Coronary CT angiography using 64 detector rows: methods and design of the multi-centre trial CORE-64. Eur Radiol 2008;19:816–828. [PubMed: 18998142]
16. Boden WE, O'Rourke RA, Teo KK, Hartigan PM, Maron DJ, Kostuk WJ, Knudtson M, Dada M, Casperson P, Harris CL, Chaitman BR, Shaw L, Gosselin G, Nawaz S, Title LM, Gau G, Blaustein AS, Booth DC, Bates ER, Spertus JA, Berman DS, Mancini GB, Weintraub WS. Optimal medical therapy with or without PCI for stable coronary disease. N Engl J Med 2007;356:1503–1516. [PubMed: 17387127]
17. Altman, DG. Practical Statistics for Medical Research. Chapman and Hall; London/New York: 1991. p. 611
18. Bland JM, Altman DG. Statistical methods for assessing agreement between two methods of clinical measurement. Lancet 1986;1:307–310. [PubMed: 2868172]
19. Zweig MH, Campbell G. Receiver-operating characteristic (ROC) plots: a fundamental evaluation tool in clinical medicine. Clin Chem 1993;39:561–577. [PubMed: 8472349]

20. Uren NG, Melin JA, De Bruyne B, Wijns W, Baudhuin T, Camici PG. Relation between myocardial blood flow and the severity of coronary-artery stenosis. N Engl J Med 1994;330:1782–1788. [PubMed: 8190154]
21. Pijls NH, De Bruyne B, Peels K, Van Der Voort PH, Bonnier HJ, Bartunek JKJJ, Koolen JJ. Measurement of fractional flow reserve to assess the functional severity of coronary-artery stenoses. N Engl J Med 1996;334:1703–1708. [PubMed: 8637515]
22. Hachamovitch R, Hayes SW, Friedman JD, Cohen I, Berman DS. Comparison of the short-term survival benefit associated with revascularization compared with medical therapy in patients with no prior coronary artery disease undergoing stress myocardial perfusion single photon emission computed tomography. Circulation 2003;107:2900–2907. [PubMed: 12771008]
23. Iskandrian AS, Chae SC, Heo J, Stanberry CD, Wasserleben V, Cave V. Independent and incremental prognostic value of exercise single-photon emission computed tomographic (SPECT) thallium imaging in coronary artery disease. J Am Coll Cardiol 1993;22:665–670. [PubMed: 8354796]
24. Lin F, Shaw LJ, Berman DS, Callister TQ, Weinsaft JW, Wong FJ, Szulc M, Tandon V, Okin PM, Devereux RB, Min JK. Multidetector computed tomography coronary artery plaque predictors of stress-induced myocardial ischemia by SPECT. Atherosclerosis 2008;197:700–709. [PubMed: 17720167]
25. Daghini E, Primak AN, Chade AR, Zhu X, Ritman EL, McCollough CH, Lerman LO. Evaluation of porcine myocardial microvascular permeability and fractional vascular volume using 64-slice helical computed tomography (CT). Invest Radiol 2007;42:274–282. [PubMed: 17414522]
26. Hsu LY, Rhoads KL, Holly JE, Kellman P, Aletras AH, Arai AE. Quantitative myocardial perfusion analysis with a dual-bolus contrast-enhanced first-pass MRI technique in humans. J Magn Reson Imaging 2006;23:315–322. [PubMed: 16463299]
27. Hoffman JI. Transmural myocardial perfusion. Prog Cardiovasc Dis 1987;29:429–464. [PubMed: 2953043]
28. Stoll M, Quentin M, Molojavyi A, Thamer V, Decking UK. Spatial heterogeneity of myocardial perfusion predicts local potassium channel expression and action potential duration. Cardiovasc Res 2008;77:489–496. [PubMed: 18006439]
29. Husmann L, Valenta I, Gaemperli O, Adda O, Treyer V, Wyss CA, Veit-Haibach P, Tatsugami F, von Schulthess GK, Kaufmann PA. Feasibility of low-dose coronary CT angiography: first experience with prospective ECG-gating. Eur Heart J 2008;29:191–197. [PubMed: 18089704]
30. Koepfli P, Wyss CA, Namdar M, Klainguti M, von Schulthess GK, Luscher TF, Kaufmann PA. Beta-adrenergic blockade and myocardial perfusion in coronary artery disease: differential effects in stenotic versus remote myocardial segments. J Nucl Med 2004;45:1626–1631. [PubMed: 15471825]
31. Kitagawa K, George RT, Chang H, Lima JA, Lardo AC. Myocardial perfusion assessment using dynamic-mode 256-row multidetector computed tomography: influence of beam hardening correction. JCCT 2008;2:S24.

Figure 1.
CT imaging protocols for 64- and 256-detector CT.

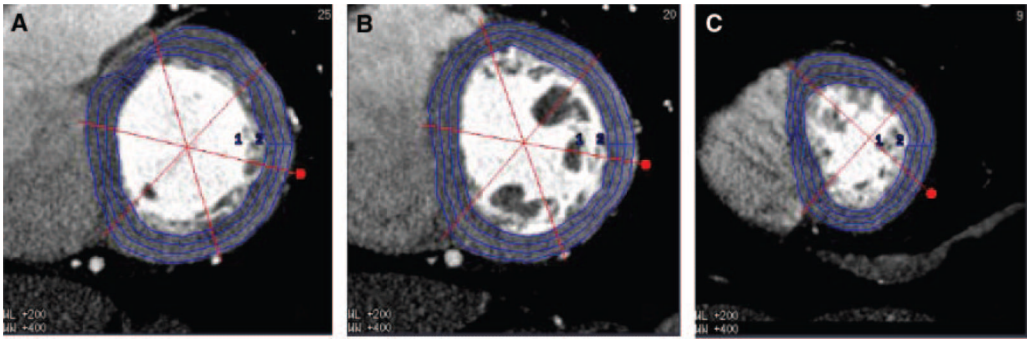

Figure 2.
Left ventricular segmentation of CTP images. A through C, 16-segment analysis of the subendocardial, midmyocardial, and subepicardial layers, excluding only the most distal apex.

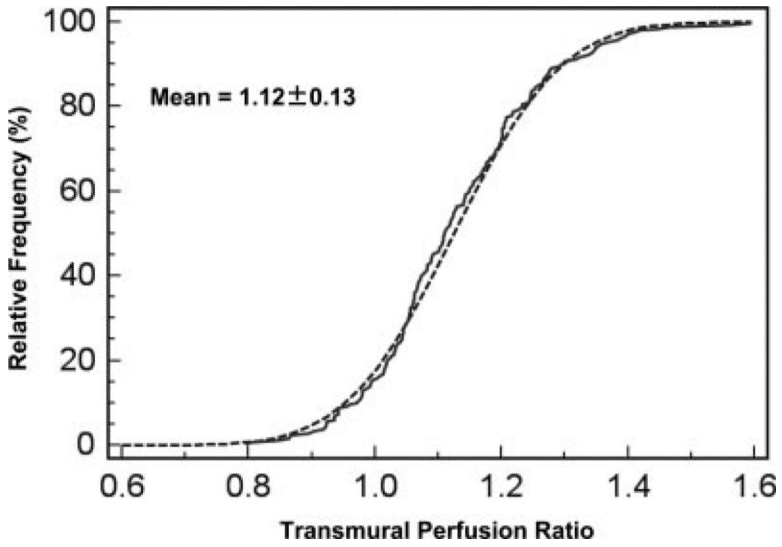

Figure 3.

Relative frequency distribution plot (solid line) of the transmural perfusion ratio (*x*-axis) measurements in patients with no obstructive atherosclerosis determined with invasive coronary angiography (n=224 myocardial segments). Dotted line represents the normal distribution.

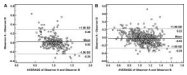

Figure 4.
Bland-Altman Plot demonstrating the agreement in the measurement of the TPR between observer A and observer B on the rest (A) and stress (B) images.

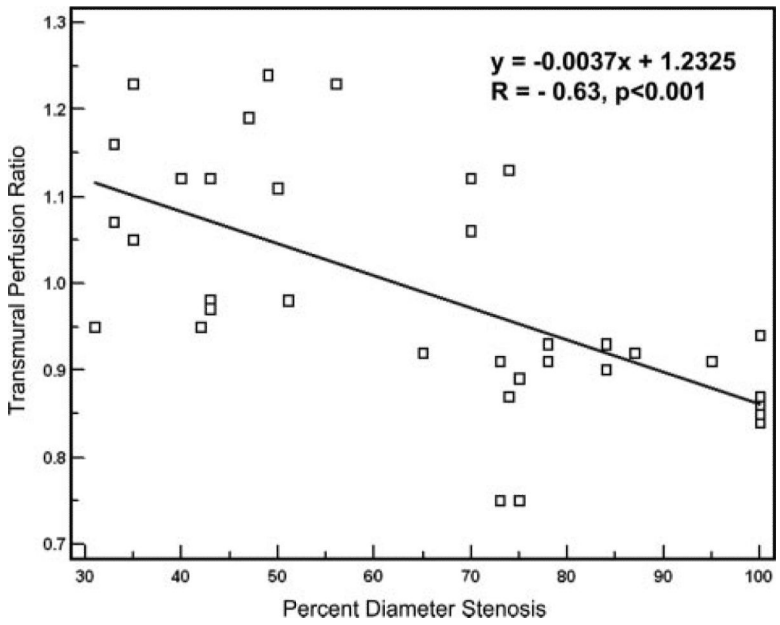

Figure 5.
TPR versus percent diameter stenosis on QCA performed on invasive coronary angiograms in patients with stenoses ≥30%.

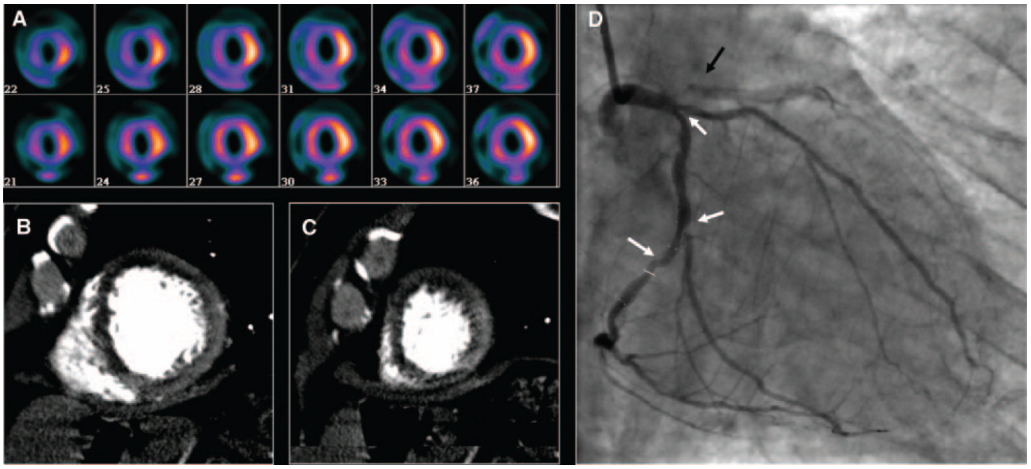

Figure 6.

Images from 64-row detector CTP. A, Partially reversible perfusion deficit in the territory of the LAD and a primarily fixed perfusion deficit in the inferior wall on radionuclide myocardial perfusion imaging with increased subdiaphragmatic tracer uptake (stress, upper panels; rest, lower panels). B and C, Adenosine stress CTP shows a dense perfusion deficit in the LAD territory, as well as a subendocardial perfusion deficit in the inferior and lateral walls. D, Invasive coronary angiogram demonstrates a left-dominant system with a totally occluded LAD (black arrow) as well as intermediate and high-grade stenoses in a large ramus intermedius, the body of the left circumflex, an the ostium of the obtuse marginal artery (white arrows).

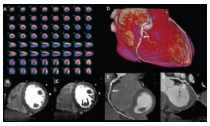

Figure 7.
Images from 256-row detector CTP. A, Partially reversible perfusion deficit in the inferior and inferolateral wall on radionuclide MPI in this patient with exertional angina (stress, upper panels; rest, lower panels). Rest (B) and stress (C) CTP imaging shows a reversible subendocardial perfusion deficit in the inferior and inferolateral walls. Noninvasive angiography confirms a significant stenoses (white arrows) in the proximal right coronary artery (D and E) and the proximal left circumflex artery (F).

Table 1

Baseline Characteristics

Age, y	60.9±10.1
Body mass index, kg/m^2	28.1±11.9
Male	28 (65)
Female	15 (35)
Tobacco use (current or prior)	24 (56)
Family history of premature CAD	12 (28)
Diabetes mellitus	12 (28)
Prior CAD	10 (23)
Known prior MI	2 (5)
Prior PTCA with stent	4 (9)
Hyperlipidemia	36 (84)
Hypertension	34 (79)
Chronic β-blocker use	22 (51)

Data are presented as mean±SD or n (%). MI indicates myocardial infarction; PTCA, percutaneous transluminal coronary angioplasty.

Table 2

Accuracy Parameters of CTA/CTP in the Per-Patient Analysis

	With Nonevaluable Vessels Categorized as Negative (n=27)	With Nonevaluable Vessels Categorized as Positive (n= 27)	Evaluable Vessels Only (n=26)
Prevalence	15/27, 56%	16/27, 59%	14/26, 54%
Sensitivity	12/15, 80% (51–95)	14/16, 88% (60–98)	12/14, 86% (57–97)
Specificity	11/12, 92% (60–100)	10/11, 91% (57–100)	11/12, 92% (61–98)
PPV	12/13, 92% (62–100)	14/15, 93% (66–100)	14/15, 92% (62–100)
NPV	11/14, 79% (49–94)	10/12, 83% (51–97)	11/13, 85% (54–97)
AUC	0.84 (0.77–0.90)	0.89 (0.71–0.97)	0.88 (0.70–0.97)

Data are presented as n/N, % (95% CI). The reference gold standard is QCA plus SPECT MPI. AUC indicates area under curve.

Table 3

Accuracy Parameters of CTA/CTP in the Per-Vessel/Territory Analysis

	With Nonevaluable Vessels Categorized as Negative (n=81)	With Nonevaluable Vessels Categorized as Positive (n= 81)	Evaluable Vessels Only (n=76)
Prevalence	18/81, 22%	18/81, 22%	16/76,21%
Sensitivity	12/18, 67% (41–86)	14/18, 78% (52–93)	12/16, 75% (47–92)
Specificity	53/63, 84% (72–92)	51/63, 81% (69–89)	52/60, 87% (75–94)
PPV	12/22, 55% (33–75)	14/26, 54% (34–73)	12/20, 60% (36–80)
NPV	53/59, 90% (79–96)	51/55, 93% (82–98)	52/56, 93% (82–98)
AUC	0.75 (0.64–0.84)	0.79 (0.68–0.87)	0.80 (0.70–0.89)
	With Nonevaluable Vessels Categorized as Negative (n= 81)	**Corrected for Multivessel Disease With Nonevaluable Vessels Categorized as Positive (n= 81)**	**Evaluable Vessels Only (n=76)**
Prevalence	21/81, 26%	21/81, 26%	19/76, 25%
Sensitivity	15/21, 71% (48–88)	17/21, 81% (57–94)	15/19, 79% (54–93)
Specificity	53/60, 88% (77–95)	51/60, 85% (73–92)	52/57, 91% (80–97)
PPV	15/22, 68% (45–85)	17/26, 65% (44–82)	15/20, 75% (51–90)
NPV	53/59, 90% (79–96)	51/55, 93% (82–98)	52/56, 93% (82–98)
AUC	0.79 (0.69–0.88)	0.83 (0.73–0.90)	0.85 (0.75–0.92)

Data are presented as n/N, % (95% CI). The reference gold standard is QCA plus SPECT MPI. The top half of the table shows data without correction for multivessel disease, and the bottom shows data with correction for multivessel disease. AUC indicates area under curve.